ORIGINAL ARTICLE

Galactosylated chitosan/5-fluorouracil nanoparticles inhibit mouse hepatic cancer growth and its side effects

Ming-Rong Cheng, Qing Li, Tao Wan, Bing He, Jiang Han, Hou-Xiang Chen, Feng-Xiao Yang, Wei Wang, Hong-Zhi Xu, Tao Ye, Bing-Bing Zha

Ming-Rong Cheng, Jiang Han, Wei Wang, Department of General Surgery, Shanghai Pudong New Area Zhoupu Hospital, Shanghai 201318, China

Qing Li, Department of General Medicine, Pujiang Branch of Shanghai Fifth People's Hospital, Shanghai 201112, China

Tao Wan, Hou-Xiang Chen, Feng-Xiao Yang, Biomedical Materials and Engineering Center, Wuhan University of Technology, Wuhan 430070, Hubei Province, China

Ming-Rong Cheng, Bing He, Hong-Zhi Xu, Tao Ye, Department of General Surgery, Shanghai Fifth People's Hospital, Fudan University, Shanghai 200240, China

Bing-Bing Zha, Department of Endocrine, Shanghai Fifth People's Hospital, Fudan University, Shanghai 200240, China

Correspondence to: Tao Wan, Associate Professor, Biomedical Materials and Engineering Center, Wuhan University of Technology, 122 Luoshi Road, Wuhan 430070, Hubei Province, China. wantao@whut.edu.cn
Telephone: +86-27-87651852 Fax: +86-27-87880734

Abstract

AIM: To observe the curative effect of galactosylated chitosan (GC)/5-fluorouracil (5-FU) nanoparticles in liver caner mice and its side effects.

METHODS: The GC/5-FU nanoparticle is a nanomaterial made by coupling GC and 5-FU. The release experiment was performed *in vitro*. The orthotropic liver cancer mouse models were established and divided into control, GC, 5-FU and GC/5-FU groups. Mice in the control and GC group received an intravenous injection of 200 μL saline and GC, respectively. Mice in the 5-FU and GC/5-FU groups received 200 μL (containing 0.371 mg 5-FU) 5-FU and GC/5-FU, respectively. The tumor weight and survival time were observed. The cell cycle and apoptosis in tumor tissues were monitored by flow cytometry. The expression of p53, Bax, Bcl-2, caspase-3 and poly adenosine 50-diphosphate-ribose polymerase 1 (PARP-1) was detected by immunohistochemistry, reverse transcription-polymerase chain reaction and Western blot. The serum blood biochemical parameters and cytotoxic activity of natural killer (NK) cell and cytotoxicity T lymphocyte (CTL) were measured.

RESULTS: The GC/5-FU nanoparticle is a sustained release system. The drug loading was 6.12% ± 1.36%, the encapsulation efficiency was 81.82% ± 5.32%, and the Zeta potential was 10.34 ± 1.43 mV. The tumor weight in the GC/5-FU group (0.4361 ± 0.1153 g *vs* 1.5801 ± 0.2821 g, $P < 0.001$) and the 5-FU (0.7932 ± 0.1283 g *vs* 1.5801 ± 0.2821 g, $P < 0.001$) was significantly lower than that in the control group; GC/5-FU treatment can significantly lower the tumor weight (0.4361 ± 0.1153 g *vs* 0.7932 ± 0.1283 g, $P < 0.001$), and the longest median survival time was seen in the GC/5-FU group, compared with the control (12 d *vs* 30 d, $P < 0.001$), GC (13 d *vs* 30 d, $P < 0.001$) and 5-FU groups (17 d *vs* 30 d, $P < 0.001$). Flow cytometry revealed that compared with the control, GC/5-FU caused a higher rate of G0-G1 arrest (52.79% ± 13.42% *vs* 23.92% ± 9.09%, $P = 0.014$) and apoptosis (2.55% ± 1.10% *vs* 11.13% ± 11.73%, $P < 0.001$) in hepatic cancer cells. Analysis of the apoptosis pathways showed that GC/5-FU upregulated the expression of p53 at both the protein and the mRNA levels, which in turn lowered the ratio of Bcl-2/Bax expression; this led to the release of cytochrome C into the cytosol

from the mitochondria and the subsequent activation of caspase-3. Upregulation of caspase-3 expression decreased the PARP-1 at both the mRNA and the protein levels, which contributed to apoptosis. 5-FU increased the levels of aspartate aminotransferase and alanine aminotransferase, and decreased the numbers of platelet, white blood cell and lymphocyte and cytotoxic activities of CTL and NK cells, however, there were no such side effects in the GC/5-FU group.

CONCLUSION: GC/5-FU nanoparticles can significantly inhibit the growth of liver cancer in mice *via* the p53 apoptosis pathway, and relieve the side effects and immunosuppression of 5-FU.

INTRODUCTION

Hepatocellular cancer (HCC) is one the most prevalent malignancies[1,2]. Liver transplantation remains the most effective therapeutic option for HCC; however, due to the lack of donors and the relatively high cost, a substantial number of patients die while waiting for a donor liver[3,4]. The disadvantages of most anti-cancer drugs that are currently available include low bioavailability, poor selectivity because they can act on both tumor cells and healthy cells, and immunosuppression that can cause complications and even patient death[5]. However, targeted therapy for HCC may be useful because it is relatively less expensive compared with the current therapies and it also produces fewer side effects[6,7]. 5-fluorouracil (5-FU) is a pyrimidine anticancer drug. Since its development by Heidelberg in 1957, 5-FU has occupied an important position in the cancer chemotherapy field. Because 5-FU is highly effective against a broad spectrum of malignancies, it is widely used in chemotherapy regimens against cancers such as hepatocellular, gastric, pancreatic and breast cancers; 5-FU is very important in the management of liver cancer. 5-FU belongs to the cell cycle specific drugs and can be converted into fluorouracil deoxynucleotide to bind with thymidine synthase, which leads to the disruption of RNA, DNA and protein biosynthesis. However, because of the similarity of the nucleic acid metabolism pathways between tumor and normal tissues, 5-FU can also target normally proliferating tissues, leading to bone marrow suppression and gastrointestinal reactions. Other disadvantages of 5-FU include irregular absorption, a short half-life, and rapid turnover, which require lengthy, high-dose intravenous administration to maintain its effective *in vivo* concentration for a suitable period[8,9]; these disadvantages can significantly restrict the clinical application of 5-FU. The emergence of a novel, sustained-release formulation of 5-FU is of clinical significance because it has fewer side effects compared to the regular 5-FU formulation[10-12]. Galactosylated chitosan (GC) is a galactose ligand, with chitosan modifications on the molecular structure[13-15]. Asialoglycoprotein receptor (ASGPR) is a receptor found on the membrane of hepatocytes facing the sinusoids, with specificity for glycoproteins with galactose or acetyl galactosamine at the end. Each hepatocyte contains approximately two million binding sites for ASGPR[16]. The binding of the galactose ligand with ASGPR induces liver-targeted gene transfer. Our lab previously synthesized a GC nanoparticle as a gene carrier and showed that the GC nanoparticle can successfully transfer genes into the liver *in vitro* and *in vivo*. We also confirmed that this nanoparticle material has a high selectivity to the liver and a low cytotoxicity[17]. In the present study, we synthesized GC/5-FU nanoparticles by combining the GC material with 5-FU, and tested its effect on liver cancer *in vitro* and *in vivo*. We found that the GC/5-FU nanoparticles can specifically target the liver and that the addition of GC increases the cytotoxicity of 5-FU and apoptosis mediated by the p53 pathway. GC/5-FU nanoparticles can ameliorate the side effects and immunosuppressive action of 5-FU.

MATERIALS AND METHODS

Reagents

Chitosan (deacetylation degree > 85%) GC was synthesized and stored by our group. HCl was from Shanghai Medpep, AR. LC-10A HPLC (Shimadzu, Japan), flow cytometry (FACS Calibunr, United States). The immunohistochemistry kit was from GBI, United States. Caspase-3 and poly ADP-ribose polymerase 1 (PARP-1) antibodies were from Santa Cruz, CA, United States; Bax and Bcl-2 antibodies were from Temecula, CA, United States; and p53 antibody was from Beverly, MA, United States.

Mice and cell lines

The mouse liver cancer cell lines (H22) were purchased from the Cancer Institute of Fudan University, China. Female BALB/c mice, 7 wk of age and weighing 25 g, were

obtained from the Department of Experimental Animals of Fudan University, China. All mice were housed in specific pathogen-free level B animal facility and animal experiments were conducted following the guidelines of the Animal Research Ethics Board of Fudan University.

Synthesis of GC/5-FU

The 5-FU/GC was mixed at a mass ratio of 10:1 in solution, using vortex oscillator (2500 r/min) for 30 s; the final concentration of 5-FU was 1.857 g/L. The product was kept at room temperature for 30 min to assess for further particle formation. The final product was kept at 4 ℃. The drug loading and encapsulation efficiency were calculated according to the following equations: drug loading = the amount of 5-FU within nanoparticle/ nanoparticle mass × 100%; encapsulation efficiency = the amount of 5-FU within nanoparticle/total amount of 5-FU added × 100%.

In vitro release experiment

GC/5-FU nanoparticles (20 mg) were mixed with 30 mL of simulated body fluid (pH 7.4) in dialysis bags and incubated at 37 ℃ using a shaker with a fixed speed of 60 r/min. Samples were taken at 0.5, 1, 2, 3, 4, 5, 6, 7, 8, 9 and 10 d after mixing. The optical density (*A*) was measured at 265 nm by an automated microplate reader (Bio-Rad Inc, California, United States). The amount of 5-FU released at different time points was calculated according to a standard absorbance curve. The concentration and cumulative release rate were calculated according to the standard curve equation. Each experiment was performed in triplicate.

Animal model

The subcutaneous liver cancer mouse model was established using the mouse HCC cell line H22. After euthanasia and dissection, fresh fast-growing tumor tissues were minced and made into a tumor cell suspension at a density of 6×10^4/L. Recipient mice were anesthetized by 20% urethane, followed by an injection of 50 μL of tumor cell suspension into the left liver lobe capsule. Approximately two min after completion of the procedure, when there was no leaking, the abdomen was sutured and the orthotropic liver cancer mouse model was established successfully[18].

Curative effect of GC/5-FU in the orthotropic liver cancer mouse model

Five days after the establishment of the orthotropic liver cancer mouse model, the tumor reached a size of about 4-6 mm in diameter (Figure 1). The mouse models were randomly assigned into 4 groups labeled as control, GC, 5-FU and GC/5-FU. Mice in the control group received an intravenous injection of 200 μL saline. GC group received 200 μL GC nano-material. 5-FU and GC/5-FU groups received 200 μL (containing 0.371 mg 5-FU) 5-FU and GC/5-FU, respectively. The drugs were given continuously for 5 d starting from day 5 after the tumor

Figure 1 Establishment of the hepatic cancer mouse model. A: Liver cancer; B: Normal mouse liver.

was established. At day 15, 10 mice were sacrificed and the tumor growth was monitored. The remaining 15 mice in each group were kept for survival analysis.

Cell cycle and apoptosis analysis by flow cytometry

The cell suspension was made of 1-2 mL tumor tissues from each individual group. Cells were washed three times by 0.1 mol/L phosphate buffered solution (PBS) and fixed by 70% ethanol. Cells were then incubated with 50 mg/L propidium iodide (Zhengzhou Sigma Chemical, Zhengzhou, China), 1.0% Triton X-100 and 10 mg/L RNaseA for 30 min at 4 ℃ in dark. Cell cycle distribution was analyzed by flow cytometry. Proliferation index (PI) = (S + G2/M)/(G0/G1 + S + G2/M). Apoptosis was determined by staining cells with annexin V-FITC (Pharmingen, San Diego, CA, United States) and propidium iodide because annexin V can identify the externalization of phosphatidylserine during the progression of apoptosis and therefore can detect early apoptotic cells. To quantify apoptosis, cells were washed twice with cold PBS and resuspended in binding buffer at 1×10^3 cells/L. A quantity of 100 μL of this suspension was transferred to a 5 mL culture tube with 5 mL of annexin V-FITC and 10 mL of 20 mL/L propidium iodide, and analyzed using the flow cytometry.

Immunohistochemistry

The 4 μm sections were deparaffinized by incubation at 65 ℃. Sections were soaked in 3% H_2O_2 for 10 min at room temperature to deactivate endogenous peroxidases. Antigen retrieval was performed using a microwave. The primary antibody was incubated at 37 ℃ for 1 h in a humidified chamber; the secondary antibody was incubated at 37 ℃ for 30 min. After washing, the sections were developed using diaminobenzidine, and counter stained with hematoxylin. After dehydration, the sections were analyzed under a light microscope[19]. p53 staining was mainly observed in the nucleus, which appeared brown and granular with little background. Caspase-3 staining was mainly present in cytoplasm, showing a brown granular staining pattern. PBS was used instead of primary antibody for a negative control. The Image-pro plus 6.0

system was used to analyze five fields randomly chosen from each slide. The images were amplified 200-fold, converted into gray-scale so as to distinguish the positive staining area from background. The positive-stained area and the total area of the field were measured by the system and the area ratio was calculated using the following equation: staining area/total area × 100%. The stained area of each individual slide was determined by averaging the area ratio.

Reverse transcription-polymerase chain reaction

Primers were purchased from Shanghai R and S Biotechnology Co., Ltd. The oligonucleotide primers used were: Bcl-2: 5'-CGGGCTGGGGGATGACTTCTCT-3' (sense), 5'-GCATCCCAGCCTCCGTTATCC-3' (antisense); Bax: 5'-AGACACCTGAGCTGACCTTGGAG-3' (sense), 5'-AGACACCTGAGCTGACCTTGGAG-3' (antisense); PARP-1: 5'-TCCCAAGGACTCCCTCCGCATGG-3' (sense), 5'-CTTTGCCTGCCACGCCTCCAGCC-3' (antisense); Caspase-3: 5'-TTGGAACAAATGGACCTG-3' (sense), 5'-ACAAAGCGACTGGATGAA-3' (antisense); P53: 5'-GTGGCCTCTGTCATCTTCCG-3' (sense), 5'-CCGTCACCATCAGAGCAACG-3' (antisense); glyceraldehyde-3-phosphate dehydrogenase (GAPDH) was used as an internal control : 5'-ACCGCAAAGACTGT-GGATGC-3' (sense), 5'-TGAGCTTGACAAAGTGG TCG-3' (antisense). Tissue total RNA was extracted by TRIZOL (Invitrogen, California, United States). Total RNA (1 μL) was used to reverse transcribe into cDNA using 0.5 μL AMV reverse transcriptase. Polymerase chain reaction (PCR) was performed using 2.5 μL cDNA, 0.1 μL Ex Taq HS, 0.1 μL forward primer and 0.1 μL reverse primer. The PCR reaction conditions were as follows: 94 ℃ for 2 min, 35 cycles of 94 ℃ for 40 s, 50 ℃ to 6 ℃ for 40 s and 72 ℃ for 1 min, followed by 72 ℃ for 5 min. PCR products were kept at -20 ℃[20]. GAPDH was used as internal control. The PCR product (6 μL) was resolved in 2% agarose gel for 30 min at 120 V, 100 mA, stained with ethidium bromide solution for 5 min, imaged by a ultraviolet gel imaging system, and analyzed by Quantity One software (Bio-Rad Inc, California, United States). The expression of target genes was presented as the ratio of target to internal control GAPDH.

Western blotting analysis

After the concentration was determined, the samples were loaded onto the 12% sodium dodecyl sulfate polyacrylamide gel electropheresis (SDS-PAGE) gel and resolved at 80 V followed by 120 V. Methanol-pretreated polyvinylidene difluoride (PVDF) membrane was then soaked in transfer buffer (pH 8.3, 25 mmol/L Tris-HCl, 192 mmol/L glycine, 20% methanol) for 10 min. Proteins on the SDS-PAGE gel were then transferred onto the PVDF membrane under 100 volts (V) for 70 min. The membrane was blocked by 5% FBS/PBS at 4 ℃ overnight. Primary antibodies were diluted at 1:2000 and incubated with a membrane for 3 min at room temperature. The membrane was then washed three times for 10

min each with PBS containing 0.05% Tween 20. Goat-anti-mouse immunoglobulin G secondary antibody (1:8000) was added to incubate with the membrane for 3 h at room temperature, followed by washing three times using the same washing solution. The membrane was then developed for 1 min using an enhanced chemiluminescence kit with equal volumes of A and B solution[21]. After imaging, Image J version 1.44 software (National Institutes of Health) was used to analyze the average density values.

Analysis of blood biochemical parameters

The animals were sacrificed by day 10 after treatment. Blood chemistry including the measurement of alanine aminotransferase (ALT), aspartate aminotransferase (AST), blood urea nitrogen and creatinine was examined by a Fuji Drychem 3500 automated analyzer (Fuji Medical System Co. Ltd., Tokyo), the blood routine such as hemoglobin (Hbg), platelet (PLT), white blood cell (WBC), lymphocyte and neutrophil was detected by a Sysmex XS-800i automated analyzer (Sysmex Shanghai Ltd, Shanghai, China) .

Cytotoxic assay for natural killer cell and cytotoxicity T lymphocyte

Natural killer cell (NK) and cytotoxicity T lymphocyte (CTL) cytotoxic activity was measured by the 3-(4, 5-dimethylthiazd-2-yl)-2,5-diphenyltentrazolium bromide (MTT) colorimetry assay (Sigma, United States) as reported previously[17]. $1 × 10^4$ YAC-1 as target cells were seeded in a 96-well plastic plates. Spleen cells used as effector cells were prepared from the mice and were simultaneously seeded in a 96-well plate at a 50:1 ratio of effector to target (E:T) in CTL assay. The effector cells from spleen cells were incubated with H22 target cells at a 50:1 ratio of E:T. All cytotoxic activity assays were performed in triplicate.

The activities of CTL and NK were calculated using the following formulas: CTL activity (%) = $[1 - (A_{E+T} - A_E)/A_T] × 100$%; NK activity (%) = $[1 - (A_{E+T} - A_E)/A_T] × 100$%, where A_E indicates the mean A value of effector cells, A_T indicates the mean A value of target cells, and A_{E+T} indicates the mean A value of effector cells + target cells.

Statistical analysis

All data was collected and expressed as mean ± SD. Analysis of variance (ANOVA) was used to analyze data within the same group, one-way ANOVA was used to analyze data between groups, while the least significant digit method was used for pairwise comparison between groups. A value of $a = 0.05$ and $P < 0.05$ was considered statistically significant.

RESULTS

Synthesis and characterization of GC/5-FU nanoparticles

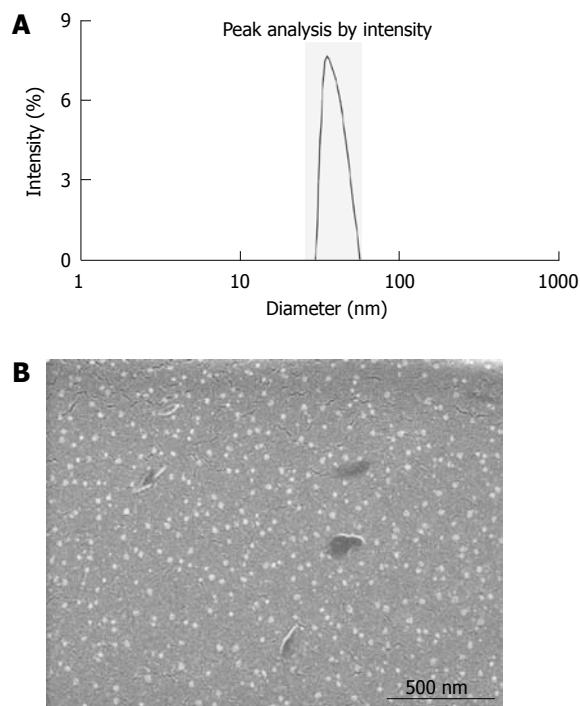5-FU/GC nanoparticles were successfully synthesized,

Figure 2 Particle size and scanning electron microscope image of galactosylated chitosan/5-fluorouracil. A: Particle size graph showing the diameter of galactosylated chitosan/5-fluorouracil (GC/5-FU) (35.19 ± 9.50 nm); B: Scanning electron microscope image of GC/5-FU. The particles show spherical structure with a smooth surface and no adhesion between nanoparticles.
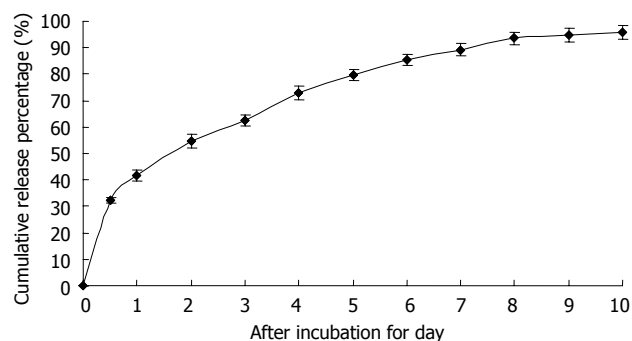

Figure 3 The *in vitro* release curve of nanoparticles in simulated body fluid (37 ℃, pH 7.4, *n* = 3). A rapid release was observed from time 0 h to 12 h, with a cumulative release percentage of 32.4%; a smooth slow-release occurred between day 1 and day 8, with a cumulative release percentage of 93.50%. During days 8 to 10, the release reached a plateau, with a cumulative release percentage of 95.70% at day 10.

and the radius of the nanoparticles was 35.19 ± 9.50 nm, which had a normal distribution (Figure 2A). Electron microscopy showed that the particles were in regular spherical shape, with a smooth surface, a uniform size, and no adhesion between nanoparticles (Figure 2B). The drug loading was 6.12% ± 1.36%, the encapsulation efficiency was 81.82% ± 5.32%, and the Zeta potential was 10.34 ± 1.43 mV. Figure 3 shows the *in vitro* release curve of nanoparticles in simulated body fluid (37 ℃, pH 7.4). A rapid release was observed from 0 h to 12 h, with a cumulative release percentage of 32.4%, presum-
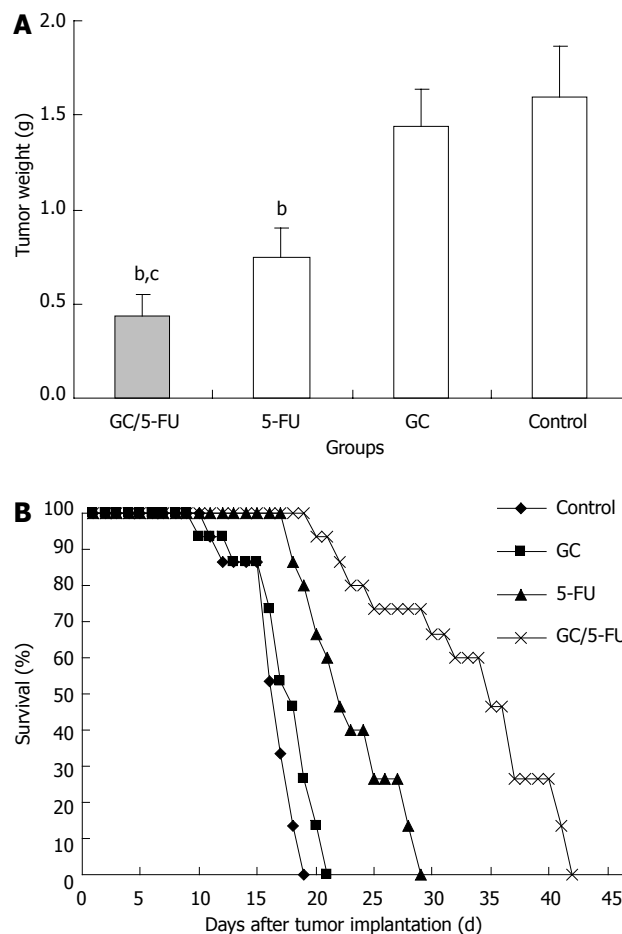

Figure 4 The curative effect of galactosylated chitosan/5-fluorouracil on liver cancer in the orthotopic transplant model of hepatocellular carcinoma. A: Five days after the tumor was established, galactosylated chitosan/5-fluorouracil (GC/5-FU), 5-FU, GC or phosphate buffered solution was given to the mice. Tumor weight was measured at day 15; B: Treatment was given as described previously and the survival was monitored. The median survival for control, GC, 5-FU and GC/5-FU groups were 12, 13, 17 and 30 d, respectively. [b]$P < 0.01$ *vs* control group; [c]$P < 0.05$ *vs* 5-FU group.

ably due to the diffusion of surface 5-FU into the solution; a smooth slow-release occurred between day 1 and day 8, with a cumulative release percentage of 93.50%, indicating that the GC/5-FU nanoparticles have a sustained release effect from days 1 to 8. From days 8 to 10, the release reached a plateau, with a cumulative release percentage of 95.70% at day 10.

Effect of GC/5-FU on tumor mass and survival in the mouse model

The tumor samples were harvested and weighted 15 d after treatment (Figure 4A). The weight of the tumor was 0.4361 ± 0.1153 g in GC/5-FU group, 0.7932 ± 0.1283 g in 5-FU group, 1.3989 ± 0.2125 g in GC group and 1.5801 ± 0.2821 g in control group. The differences between the groups was statistically significant ($P < 0.01$). The tumor weight in the GC/5-FU and the 5-FU groups were significantly lower than in the GC group and control group ($P < 0.01$) while tumor weight in the GC/5-FU group was significantly lower than in the 5-FU group ($P < 0.01$);

however, the tumor weight in the GC group and the control group was not different ($P > 0.05$). After the model was developed, the mice were randomly assigned to four groups with 15 mice each, and treated as described above. The survival of the mice was monitored, and there was a 100% mortality in all groups. The Kaplan-Meier survival curve (Figure 4B) showed that mice all the mice in the control group died between day 6 and day 14, with a median survival time of 12 d. In the GC group, all mice died between day 5 and day 16, the median survival time being 13 d. There was no statistical difference in the survival time between the control and the GC groups ($P > 0.05$). Mice treated with 5-FU also all died between day 13 and day 24, with a median survival of 17 d. All mice in the GC/5-FU group died between day 15 and day 37, with a median survival time of 30 d. The median survival time of mice treated with either 5-FU or GC/5-FU was significantly longer than that of mice in the GC or control groups; the longest median survival time was seen in the GC/5-FU group ($P < 0.01$ compared with the control, GC and 5-FU groups).

Effect of GC/5-FU on cell cycle, proliferation and apoptosis of H22 cells

Flow cytometry was used to analyze the liver cancer samples harvested 15 d after beginning the treatment. As shown in Figure 5A and B, the percentage of cells in the G0-G1 phases was significantly higher in the GC/5-FU- and 5-FU-treated tumors ($P < 0.01$), while the PI was lower than that in the GC and control groups ($P < 0.01$), suggesting that GC/5-FU and 5-FU had an overt antiproliferative effect and arrested the tumor cells in the G0-G1 phases. The percentage of apoptotic cells in the GC/5-FU and 5-FU groups was significantly increased when compared with that in the control and GC groups ($P < 0.01$). Also, the percentage of apoptotic cells of GC/5-FU group was higher than that in the 5-FU group ($P < 0.01$), suggesting that GC is able to enhance the cellular influx of 5-FU, thereby improving the pro-apoptotic effect of 5-FU (Figure 5C).

GC/5-FU induced hepatic cancer cell apoptosis via activating the p53 pathway

To understand which pathway(s) mediated the GC/5-FU-induced apoptosis, we examined the expression of p53 at both protein and mRNA levels. Compared with the control and GC groups, the expression of p53 was increased in the 5-FU and GC/5-FU groups, with the highest increase seen in the GC/5-FU group ($P < 0.01$, Figures 6, 7A and B). The ratio of Bcl-2/Bax showed a decreasing tendency from control to GC to 5-FU to GC/5-FU groups ($P < 0.01$, Figure 7D); specifically, the ratio in 5-FU and GC/5-FU was significantly lower than that in the control and GC groups, with a lowest ratio observed in the GC/5-FU group ($P < 0.01$). GC/5-FU can also significantly induce the expression of caspase-3 in the tumor tissues ($P < 0.01$, Figures 6, 7A and B). The expression of PARP-1 also displayed a decreasing ten-

dency from control to GC to 5-FU to GC/5-FU groups ($P < 0.01$, Figure 7C), with the most significant reduction seen in the GC/5-FU group. Therefore, it is likely that GC/5-FU was involved in upregulating the genes in the p53 pathway.

Side effects of GC/5-FU

In order to understand the side effect of liver and kidney function and blood cells, we examined the blood of the mouse model by day 10 after treatment. The levels of AST and ALT in 5-FU group were obviously higher than those in control group ($P < 0.01$), while those in GC/5-FU group were lower compared with 5-FU group ($P < 0.01$), there were no differences among control, GC and GC/5-FU groups ($P > 0.05$). The numbers of PLT, WBC and lymphocyte in 5-FU group were decreased more obviously as compared with the control, GC and GC/5-FU groups ($P < 0.05$ or < 0.01), however, there were no differences among these three groups ($P > 0.05$). The levels of blood urea nitrogen, creatinine, Hbg and neutrophil were approximate in different groups ($P > 0.05$), as shown in Table 1.

Cytotoxic activities of CTL and NK in mice

We evaluated whether the GC/5-FU could affect the activity of CTL and NK *in vivo* in mouse model. The harvested splenocytes were washed with PBS. The activity of CTL and NK was detected by MTT colorimetry. Figure 8 shows that the cytotoxic activities of CTL and NK cells were significantly decreased in 5-FU group compared with other three groups ($P < 0.01$), while the crosscurrent was found in GC group compared with 5-FU group ($P < 0.05$). There were no differences between control and GC/5-FU groups. These results thus demonstrate that the GC/5-FU nanoparticles could ameliorate the decreased cytotoxic activities of CTL and NK in 5-FU group.

DISCUSSION

The utilization of nanotechnology and nano-materials in the pharmaceutical field gave rise to the drug-nanoparticle carrier-release system, which is a drug delivery system using nanoparticles as the drug carriers. A particle ranging from 0.1 nm to 100 nm is considered to be a nanoparticle[22]. The size of a nanoparticle is very important for drug delivery, as the spaces between the cells in various tissues are different: it is now known that the aperture of vascular endothelial within most normal tissues is 2 nm, the aperture of the postcapillary venule is 6 nm, while that of non-continuous tumor blood vessels ranges from 100 nm to 780 nm[23,24]. The size of the nanoparticles used in this study was approximately 35.19 nm (Figure 2A), which is smaller than most nanoparticles reported[25], allowing them to enter the space within tumor cells but restricting them from penetrating the normal tissues. Scanning electron microscopy revealed a spherical structure with a smooth surface and no adhe-
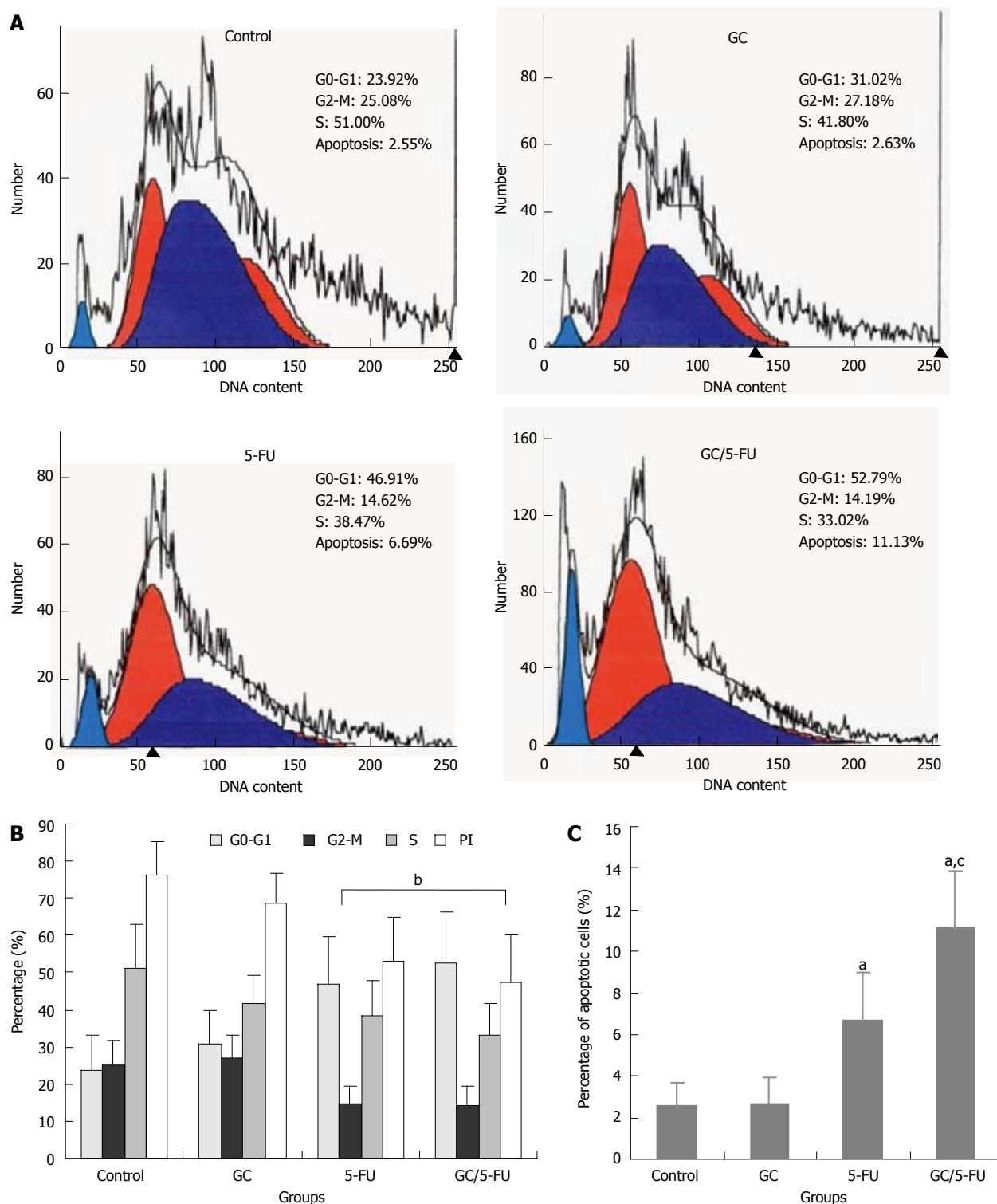
Figure 5 The effects of different treatments on cell cycle, proliferation index and apoptosis index. A: Flow cytometry analysis of cell cycle distribution of mouse liver cancer cell line (H22) cells; B: Quantification of cell cycle distribution and proliferation index of H22 cells. Percentage of cells in G0-G1 in the galactosylated chitosan/5-fluorouracil (GC/5-FU) and 5-FU groups was higher than that in control and GC groups, while the proliferation index (PI) decreased significantly ($P < 0.01$); C: Quantification of apoptosis of H22 in different treatment groups. [a]$P < 0.05$, [b]$P < 0.01$ *vs* control group; [c]$P < 0.05$ *vs* 5-FU group.

sion between nanoparticles (Figure 2B), which is consistent with previous reports[25,26]. In order to confirm the sustained release effect, we performed an experiment on GC/5-FU. The *in vitro* release curve of GC/5-FU in simulated body fluid showed that the sustained release of the nanoparticle lasted 1-8 d. Such sustained release

effect makes the drug evenly distribute in the body, thereby increasing the half-life of GC/5-FU in the circulation system and decreasing the toxic effects of 5-FU on normal tissues[27].

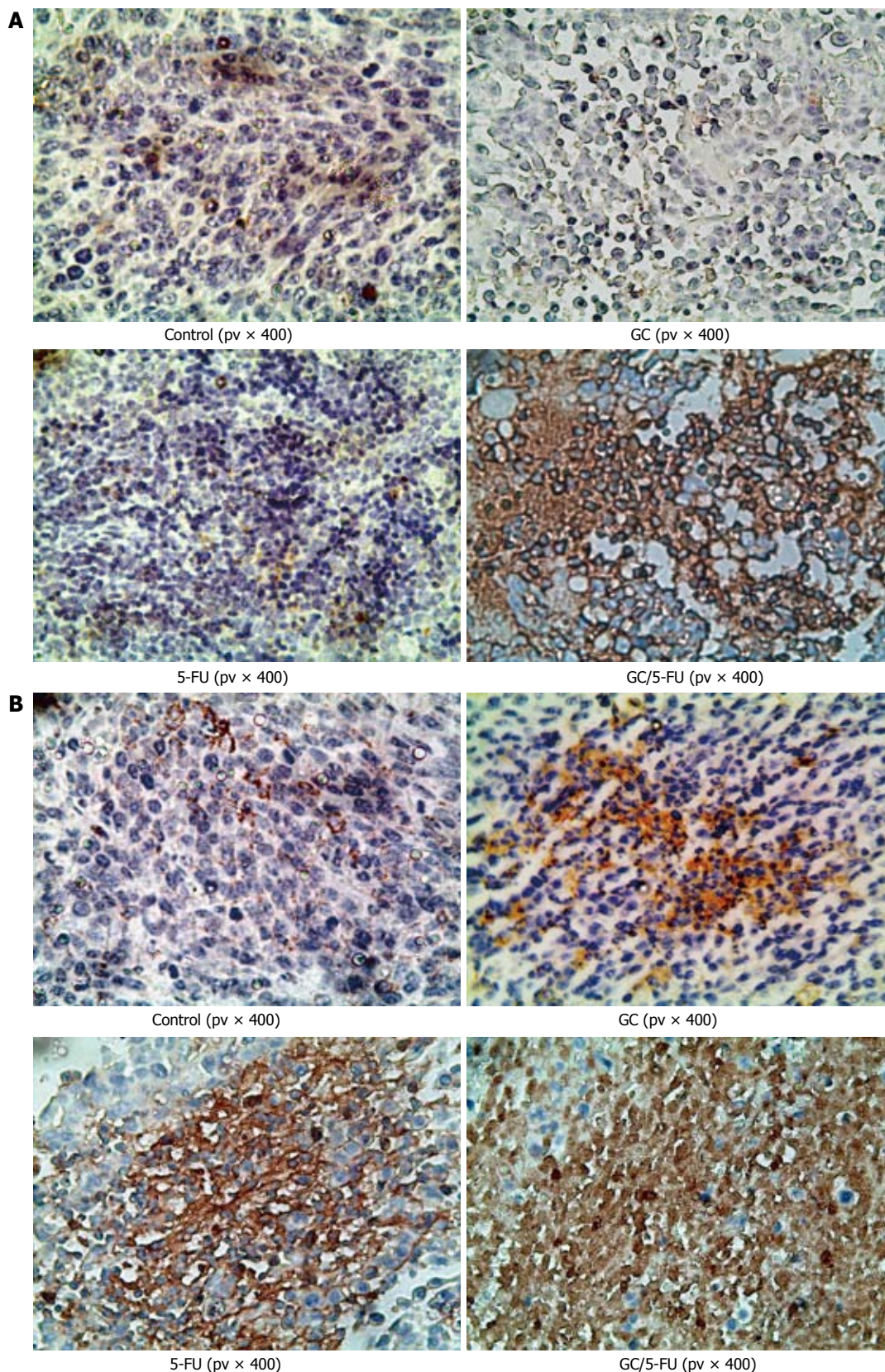In order to evaluate the curative efficiency of intravenously injected GC/5-FU in a liver cancer mouse model,

Figure 6 Immunohistochemistry of p53 and caspase-3 in the tumor sections from mice with different treatments. A: p53 staining in the control and galacto-sylated chitosan (GC) groups showed a scattered nuclear distribution pattern, in dark yellow or dark brown; while in 5-fluorouracil (5-FU) and GC/5-FU groups, p53 showed a sheet staining pattern, which was more dramatic; B: Caspase-3 staining in the control and GC groups showed a scattered cytoplasmic distribution pattern, in dark yellow or dark brown; while in 5-FU and GC/5-FU groups, caspase-3 showed a sheet staining pattern, which was more dramatic in the GC/5-FU group.
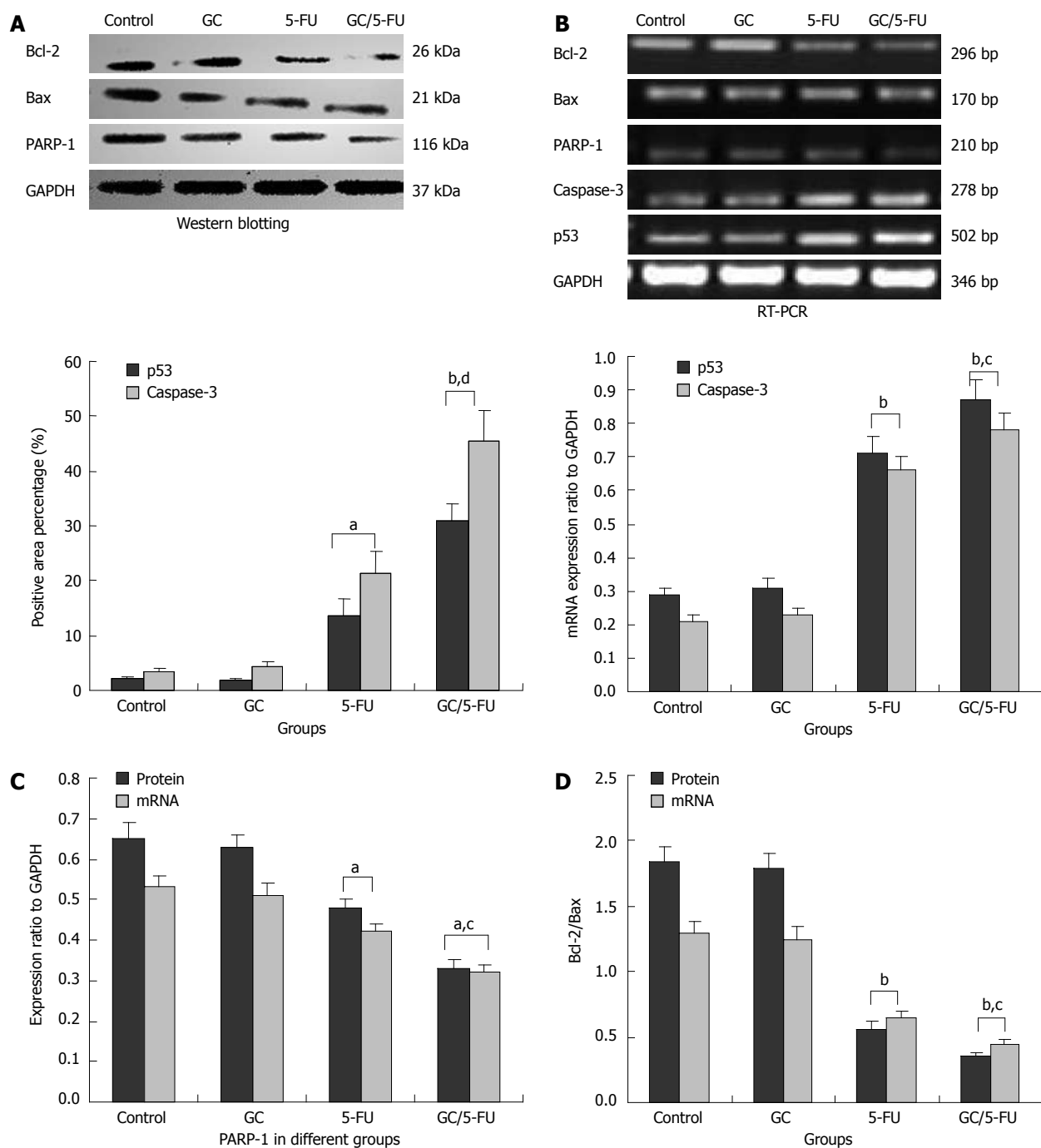
Figure 7 Expression of p53, caspase-3, Bax, Bcl-2 and poly adenosine 50-diphosphate-ribose polymerase 1 in the tumor tissues from mice with different treatments. A: Quantification of p53 and caspase-3 expression as detected by immunohistochemistry and shown pictorially in Figures 6 and 7; B: mRNA levels of p53 and caspase-3 in individual tissues was measured by reverse transcription-polymerase chain reaction (RT-PCR), and normalized to glyceraldehyde-3-phosphate dehydrogenase (GAPDH); C: Poly adenosine 50-diphosphate-ribose polymerase 1 (PARP-1) expression in individual tumor samples was determined by both RT-PCR and western blot analysis; results were normalized to GAPDH; D: Expression of Bcl-2 and Bax was quantified by both RT-PCR and Western blotting; the ratio of Bcl-2/Bax was shown. [a]$P < 0.05$, [b]$P < 0.01$ *vs* control group; [c]$P < 0.05$, [d]$P < 0.01$ *vs* 5-fluorouracil (5-FU) group. GC: Galactosylated chitosan.

some of the mice were sacrificed and analyzed at day 15. As shown in Figure 4A, the tumor weight in mice treated with GC/5-FU and 5-FU was significantly less than that in the mice treated with GC or in the control; the weight of GC/5-FU-treated tumors was even lower than the 5-FU-treated tumors, while the GC- or control-treated tumors did not show any statistically significant difference. All mice died after treatment. In the control group,

mice died between day 6 and day 14, with a median survival of 12 d; in the GC group, mice died between day 5 and day 16, with a median survival of 13 d, showing no difference from the control group (Figure 4B, $P > 0.05$). Mice in the 5-FU group succumbed to a tumor-associated death between day 13 and day 24, with a median survival time of 17 d, while mice in the GC/5-FU group died between day 15 and day 37, with a median survival

Table 1 Serum levels of blood biochemical parameters in different groups by day 10

Groups	AST (U/L)	ALT (U/L)	BUN (mmol/L)	Creatinine (μmol/L)	Hbg (g/L)	PLT (×10⁹/L)	WBC (×10⁹/L)	Lymphocyte (×10⁹/L)	Neutrophil (×10⁹/L)
Control	92.79 ± 8.74	49.73 ± 4.83	23.74 ± 5.84	0.23 ± 0.09	117.32 ± 9.87	69.43 ± 8.94	6.32 ± 1.24	3.86 ± 1.34	2.18 ± 0.73
GC	92.34 ± 7.65[d]	49.89 ± 5.13[d]	23.25 ± 6.54	0.24 ± 0.08	118.823 ± 10.85	71.43 ± 6.54[d]	6.53 ± 1.32[d]	3.95 ± 1.35[d]	2.17 ± 0.68
5-FU	113.25 ± 7.65[b]	81.48 ± 6.81[b]	23.64 ± 5.45	0.25 ± 0.07	109.41 ± 10.73	55.63 ± 7.43[a]	3.83 ± 1.18[b]	1.57 ± 1.20[a]	2.75 ± 0.87
GC/5-FU	93.42 ± 8.32[d]	48.97 ± 4.93[d]	22.94 ± 5.26	0.24 ± 0.05	116.38 ± 8.53	68.64 ± 7.38[c]	6.21 ± 1.04[d]	3.81 ± 1.17[c]	2.17 ± 0.71
F value	8.227	33.222	0.020	0.058	0.868	4.349	5.498	4.249	0.712
P value	0.002	0.000	1.012	0.941	0.482	0.018	0.008	0.024	0.526

Data were expressed as mean ± SD. *n* = 5 in each group. [a]*P* < 0.05, [b]*P* < 0.01 *vs* control group; [c]*P* < 0.05, [d]*P* < 0.01 *vs* 5-fluorouracil group. AST: Aspartate aminotransferase; ALT: Alanine aminotransferase; BUN: Blood urea nitrogen; Hbg: Hemoglobin; PLT: Platelet; WBC: White blood cell; GC: Galactosylated chitosan; 5-FU: 5-fluorouracil.
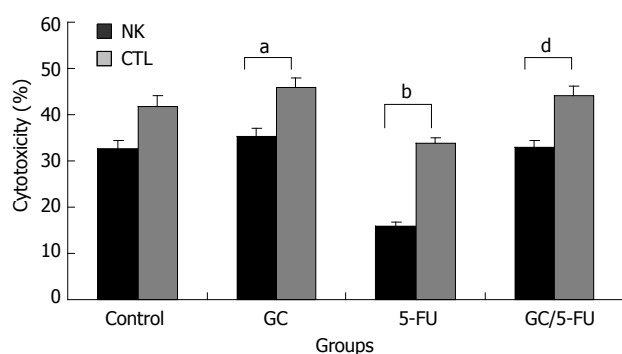

Figure 8 The activity of cytotoxicity T lymphocyte and natural killer cell was detected by 3-(4, 5-dimethylthiazd-2-yl)-2,5-diphenyltentrazolium bromide in the orthotopic transplant model of hepatocellular carcinoma. The cytotoxic activities of cytotoxicity T lymphocyte (CTL) and natural killer (NK) cells were significantly decreased in 5-fluorouracil (5-FU) group compared with other three groups (*P* < 0.01), while, the crosscurrent was found in galactosylated chitosan (GC) group compared with 5-FU group (*P* < 0.05). [a]*P* < 0.05, [b]*P* < 0.01 *vs* control group; [d]*P* < 0.01 *vs* 5-FU group.

time of 30 d. The survival time of mice treated with either 5-FU or GC/5-FU was significantly longer than that of mice in the control and GC groups, with the longest survival time seen in the GC/5-FU group. This result suggested that although GC alone cannot affect tumor growth, the conjugation of GC to 5-FU improved the tumor suppressive effect of 5-FU. To determine the mechanism of effect of GC/5-FU nanoparticles on the hepatic cancer, we used flow cytometry to examine tumor cell apoptosis. The results revealed that both 5-FU and GC/5-FU enhanced apoptosis when compared with either control or GC, and compared with 5-FU alone, GC/5-FU further increased the apoptosis index, suggesting that GC improves the pro-apoptotic effect of 5-FU by promoting its entry into the cells. In addition, as shown in Figure 5A and B, compared with control and GC treatment, 5-FU and GC/5-FU can increase the percentage of cells in the G0-G1 phases, but lower the PI, suggesting 5-FU and GC/5-FU are cytotoxic to the proliferating cells by arresting them in the G0-G1 phases; this is consistent with previously reported research[28,29]. Therefore, GC facilitates intracellular transport of 5-FU, improving the effects of 5-FU on tumor cell apoptosis and on inhibition of the cell cycle.

To further study whether the apoptosis induced by the GC/5-FU nanoparticles was mediated by the p53 pathway, we used immunohistochemistry, reverse transcription-PCR and Western blotting analysis to examine the expression of p53, Bax, Bcl-2, caspase-3 and PARP-1. We found that the addition of GC/5-FU and 5-FU induced p53 expression at both the protein and the RNA levels; the strongest induction of p53 was noted in the GC/5-FU group, and a moderate to strong induction seen in the 5-FU group (Figure 7A and B). The change of Bcl-2/Bax ratio also showed a similar pattern. Administration of GC/5-FU and 5-FU decreased the Bcl-2/Bax ratio, with the most dramatic reduction observed in the GC/5-FU group (Figure 7D). It is now known that Bax, belonging to the Bcl-2 family, is able to promote apoptosis. Although both Bax and Bcl-2 coexist in cells as dimers, each suppresses the function of the other. Physiologically, both Bax and Bcl-2 are present in cells in the same amounts, ensuring the normal growth of the cells. If Bcl-2 is overexpressed, the heterodimer Bcl-2/Bax is induced to suppress apoptosis, while if the level of Bax increases, the formation of Bax/Bax homodimer promotes apoptosis by antagonizing the anti-apoptotic effect of Bcl-2[30]. Wild-type p53 induces Bax synthesis to mediate apoptosis, while mutant p53 can inhibit apoptosis leading to uncontrolled proliferation[31]. We also found that GC/5-FU was able to significantly enhance the expression of caspase-3 (*P* < 0.01), which is known to be an important promoter of apoptosis. Caspase-3 can be activated by cytochrome c in the cytosol, which is released from mitochondria under the control of Bax and Bcl-2. Therefore, the ratio of Bax and Bcl-2 determines the activation of caspase-3[32,33]. Figure 7C shows a tendency toward a decrease in PARP-1 expression from the control to the GC to the 5-FU to the GC/5-FU groups, with a most significant reduction in the GC/5-FU group. It has been reported that caspase-3 is a pivotal effecter in apoptosis. Activation of PARP-1 after severe DNA damages results in depletion of cellular energy. In order to prevent the consumption of NAD+ and adenosine triphosphate, activated caspase-3 cleaves and inactivates PARP-1, leading to apoptosis[34]. Taking into consideration all the above results, GC improved the apoptotic effect of 5-FU in hepatic cancer cells. The mechanism underlying GC/5-FU nanoparticle-induced apoptosis was

inducing the expression of p53 at the protein and mRNA levels. The elevated p53 level can significantly lower the Bcl-2/Bax ratio which in turn promotes the release of cytochrome c from the mitochondria into the cytosol, leading to the activation of caspase-3. Upregulation of the caspase-3 gene and protein contributed to the reduction of PARP-1 at both the protein and mRNA levels, thus triggering apoptosis. Therefore, GC/5-FU-induced apoptosis is p53 dependent.

5-FU is a common chemotherapy drug, and its common side effects are the suppression of bone marrow[35], dysfunction of liver and kidney and suppression of immune function[36-38], leading to a decreased efficacy and survival time of the patients with cancer. In this experiment, 5-FU increased significantly the levels of AST and ALT, decreased obviously the numbers of PLT, WBC and lymphocyte in tumor-bearing mice compared with the control group. The levels of ALT and AST, the numbers of PLT, WBC and lymphocyte, remained stable in GC/5-FU group compared with control group. It is indicated that GC nanoparticles can improve the damage of liver function caused by 5-FU and the suppression state of bone marrow. We found that the cytotoxic activities of CTL and NK cells by 5-FU were significantly inhibited, and the GC nanoparticles could relieve the suppression state of NK and CTL cells by 5-FU, which is consistent with our previously reported experiments which verified that GC nanoparticles can stimulate the cytotoxic activities of CTL and NK cells in tumor-bearing mice[17]. So the GC/5-FU nanoparticles can alleviate the inhibition of 5-FU on the body's immunity.

In conclusion, we demonstrated that GC is a good carrier for nano-material, especially 5-FU. GC/5-FU nanoparticles had a sustained release effect. GC/5-FU nanoparticles can also significantly inhibit the tumor growth in the orthotropic liver cancer mouse model, and this *in vivo* effect was stronger than that of 5-FU alone. The mechanism underlying GC/5-FU nanoparticles may be the elevated G0-G1 arrest and apoptosis mediated by the p53 pathway. GC/5-FU nanoparticles can ameliorate the side effects and immunosuppressive action of 5-FU.

COMMENTS

Background
Biodegradable polymer nanoparticle drug delivery systems are characterized by targeted drug delivery, improved pharmacokinetic and biodistribution, enhanced drug stability and reduced side effects. These drug delivery systems are widely used for delivery of cytotoxic agents. The galactosylated chitosan (GC)/5-fluorouracil (5-FU) nanoparticle is a nanomaterial made by coupling GC, a polymer known to have the advantages described above, and 5-FU.

Research frontiers
5-FU can target normal, proliferating tissues, but with side effects of bone marrow suppression and gastrointestinal reactions. Targeted therapy for hepatocellular cancer may be useful because it is relatively less expensive compared with the current therapies and it also has fewer side effects. The emergence of a novel, sustained-release formulation of 5-FU is of clinical significance because it has fewer side effects compared with the regular 5-FU formulation.

Innovations and breakthroughs
In this paper, the authors examined the effects of GC/5-FU nanoparticle on liver cancer mouse model. As a result, GC/5-FU treatment could significantly lower the tumor weight and increase the survival time of mice when compared with 5-FU treatment alone. In addition, it was suggested that the abovementioned effects of GC/5-FU was associated with G0-G1 arrest and apoptosis of tumor cells mediated by p53 pathway. GC/5-FU nanoparticles can relieve the side effects and immune-suppressive action of 5-FU.

Terminology
The effects of GC/5-FU nanoparticle on liver cancer mouse model. GC is a galactose ligand, with chitosan modifications on the molecular structure. Asialoglycoprotein receptor (ASGPR) is a receptor found on the membrane of hepatocytes facing the sinusoids, with specificity for glycoproteins with galactose or acetyl galactosamine at the end. The galactose ligand with ASGPR in GC/5-FU nanoparticle induces liver-targeted 5-FU transfer.

Peer review
The significance of this study is evident because the improvement of chemotherapy for liver cancer is an important subject in the clinical setting. In addition, the animal experiments were generally performed appropriately.

REFERENCES

1   **Gordon-Weeks AN**, Snaith A, Petrinic T, Friend PJ, Burls A, Silva MA. Systematic review of outcome of downstaging hepatocellular cancer before liver transplantation in patients outside the Milan criteria. *Br J Surg* 2011; **98**: 1201-1208

2   **Kanwal F**, Befeler A, Chari RS, Marrero J, Kahn J, Afdhal N, Morgan T, Roberts L, Mohanty SR, Schwartz J, Vanthiel D, Li J, Zeringue A, Di'bisceglie A. Potentially curative treatment in patients with hepatocellular cancer-results from the liver cancer research network. *Aliment Pharmacol Ther* 2012; **36**: 257-265

3   **Doyle MB**, Vachharajani N, Maynard E, Shenoy S, Anderson C, Wellen JR, Lowell JA, Chapman WC. Liver transplantation for hepatocellular carcinoma: long-term results suggest excellent outcomes. *J Am Coll Surg* 2012; **215**: 19-28; discussion 28-30

4   **Li SF**, Hawxby AM, Kanagala R, Wright H, Sebastian A. Liver transplantation for hepatocellular carcinoma: indications, bridge therapy and adjuvant therapy. *J Okla State Med Assoc* 2012; **105**: 12-16

5   **Nussbaumer S**, Bonnabry P, Veuthey JL, Fleury-Souverain S. Analysis of anticancer drugs: a review. *Talanta* 2011; **85**: 2265-2289

6   **Hossain DM**, Bhattacharyya S, Das T, Sa G. Curcumin: the multi-targeted therapy for cancer regression. *Front Biosci* (Schol Ed) 2012; **4**: 335-355

7   **Manchun S**, Dass CR, Sriamornsak P. Targeted therapy for cancer using pH-responsive nanocarrier systems. *Life Sci* 2012; **90**: 381-387

8   **Rougier P**, Lepere C. Second-line treatment of patients with metastatic colorectal cancer. *Semin Oncol* 2005; **32**: S48-S54

9   **Lièvre A**, Samalin E, Mitry E, Assenat E, Boyer-Gestin C, Lepère C, Bachet JB, Portales F, Vaillant JN, Ychou M, Rougier P. Bevacizumab plus FOLFIRI or FOLFOX in chemotherapy-refractory patients with metastatic colorectal cancer: a retrospective study. *BMC Cancer* 2009; **9**: 347

10 **Rokhade AP**, Shelke NB, Patil SA, Aminabhavi TM. Novel hydrogel microspheres of chitosan and pluronic F-127 for controlled release of 5-fluorouracil. *J Microencapsul* 2007; **24**: 274-288

11 **Yan S**, Zhu J, Wang Z, Yin J, Zheng Y, Chen X. Layer-by-layer assembly of poly(L-glutamic acid)/chitosan microcapsules for high loading and sustained release of 5-fluorouracil. *Eur J Pharm Biopharm* 2011; **78**: 336-345

12 **Kevadiya BD**, Patel TA, Jhala DD, Thumbar RP, Brahmbhatt H, Pandya MP, Rajkumar S, Jena PK, Joshi GV, Gadhia PK, Tripathi CB, Bajaj HC. Layered inorganic nanocomposites: a promising carrier for 5-fluorouracil (5-FU). *Eur J Pharm Biopharm* 2012; **81**: 91-101

13 **Yang W**, Mou T, Guo W, Jing H, Peng C, Zhang X, Ma Y, Liu B. Fluorine-18 labeled galactosylated chitosan for asialo-

glycoprotein-receptor-mediated hepatocyte imaging. *Bioorg Med Chem Lett* 2010; **20**: 4840-4844

14 **Jiang H**, Wu H, Xu YL, Wang JZ, Zeng Y. Preparation of galactosylated chitosan/tripolyphosphate nanoparticles and application as a gene carrier for targeting SMMC7721 cells. *J Biosci Bioeng* 2011; **111**: 719-724

15 **Alex SM**, Rekha MR, Sharma CP. Spermine grafted galactosylated chitosan for improved nanoparticle mediated gene delivery. *Int J Pharm* 2011; **410**: 125-137

16 **Fallon RJ**, Danaher M, Saxena A. The asialoglycoprotein receptor is associated with a tyrosine kinase in HepG2 cells. *J Biol Chem* 1994; **269**: 26626-26629

17 **Cheng M**, Li Q, Wan T, Hong X, Chen H, He B, Cheng Z, Xu H, Ye T, Zha B, Wu J, Zhou R. Synthesis and efficient hepatocyte targeting of galactosylated chitosan as a gene carrier in vitro and in vivo. *J Biomed Mater Res B Appl Biomater* 2011; **99**: 70-80

18 **Chang CJ**, Chen YH, Huang KW, Cheng HW, Chan SF, Tai KF, Hwang LH. Combined GM-CSF and IL-12 gene therapy synergistically suppresses the growth of orthotopic liver tumors. *Hepatology* 2007; **45**: 746-754

19 **Rojiani MV**, Alidina J, Esposito N, Rojiani AM. Expression of MMP-2 correlates with increased angiogenesis in CNS metastasis of lung carcinoma. *Int J Clin Exp Pathol* 2010; **3**: 775-781

20 **Shi Y**, Zheng L, Luo G, Wei J, Zhang J, Yu Y, Feng Y, Li M, Xu N. Expression of zinc finger 23 gene in human hepatocellular carcinoma. *Anticancer Res* 2011; **31**: 3595-3599

21 **Li P**, Wang SS, Liu H, Li N, McNutt MA, Li G, Ding HG. Elevated serum alpha fetoprotein levels promote pathological progression of hepatocellular carcinoma. *World J Gastroenterol* 2011; **17**: 4563-4571

22 **Li DC**, Zhong XK, Zeng ZP, Jiang JG, Li L, Zhao MM, Yang XQ, Chen J, Zhang BS, Zhao QZ, Xie MY, Xiong H, Deng ZY, Zhang XM, Xu SY, Gao YX. Application of targeted drug delivery system in Chinese medicine. *J Control Release* 2009; **138**: 103-112

23 **Whitesides GM**. The 'right' size in nanobiotechnology. *Nat Biotechnol* 2003; **21**: 1161-1165

24 **Marcucci F**, Lefoulon F. Active targeting with particulate drug carriers in tumor therapy: fundamentals and recent progress. *Drug Discov Today* 2004; **9**: 219-228

25 **Song B**, Zhang W, Peng R, Huang J, Nie T, Li Y, Jiang Q, Gao R. Synthesis and cell activity of novel galactosylated chitosan as a gene carrier. *Colloids Surf B Biointerfaces* 2009; **70**: 181-186

26 **Gan Q**, Wang T, Cochrane C, McCarron P. Modulation of surface charge, particle size and morphological properties of chitosan-TPP nanoparticles intended for gene delivery. *Colloids Surf B Biointerfaces* 2005; **44**: 65-73

27 **Kim JH**, Kim YS, Park K, Lee S, Nam HY, Min KH, Jo HG, Park JH, Choi K, Jeong SY, Park RW, Kim IS, Kim K, Kwon IC. Antitumor efficacy of cisplatin-loaded glycol chitosan nanoparticles in tumor-bearing mice. *J Control Release* 2008; **127**: 41-49

28 **Sasaki K**, Tsuno NH, Sunami E, Tsurita G, Kawai K, Okaji Y, Nishikawa T, Shuno Y, Hongo K, Hiyoshi M, Kaneko M, Kitayama J, Takahashi K, Nagawa H. Chloroquine potentiates the anti-cancer effect of 5-fluorouracil on colon cancer cells. *BMC Cancer* 2010; **10**: 370

29 **Huang Z**, Guo KJ, Guo RX, He SG. Effects of 5-fluorouracil combined with sulfasalazine on human pancreatic carcinoma cell line BxPC-3 proliferation and apoptosis in vitro. *Hepatobiliary Pancreat Dis Int* 2007; **6**: 312-320

30 **Parikh N**, Koshy C, Dhayabaran V, Perumalsamy LR, Sowdhamini R, Sarin A. The N-terminus and alpha-5, alpha-6 helices of the pro-apoptotic protein Bax, modulate functional interactions with the anti-apoptotic protein Bcl-xL. *BMC Cell Biol* 2007; **8**: 16

31 **Avraam K**, Pavlakis K, Papadimitriou C, Vrekoussis T, Panoskaltsis T, Messini I, Patsouris E. The prognostic and predictive value of ERCC-1, p53, bcl-2 and bax in epithelial ovarian cancer. *Eur J Gynaecol Oncol* 2011; **32**: 516-520

32 **Lee JS**, Jung WK, Jeong MH, Yoon TR, Kim HK. Sanguinarine induces apoptosis of HT-29 human colon cancer cells via the regulation of Bax/Bcl-2 ratio and caspase-9-dependent pathway. *Int J Toxicol* 2012; **31**: 70-77

33 **Choi BH**, Kim W, Wang QC, Kim DC, Tan SN, Yong JW, Kim KT, Yoon HS. Kinetin riboside preferentially induces apoptosis by modulating Bcl-2 family proteins and caspase-3 in cancer cells. *Cancer Lett* 2008; **261**: 37-45

34 **Parkpian V**, Verasertniyom O, Vanichapuntu M, Totemchokchyakarn K, Nantiruj K, Pisitkul P, Angchaisuksiri P, Archararit N, Rachakom B, Ayurachai K, Janwityanujit S. Specificity and sensitivity of anti-beta2-glycoprotein I as compared with anticardiolipin antibody and lupus anticoagulant in Thai systemic lupus erythematosus patients with clinical features of antiphospholipid syndrome. *Clin Rheumatol* 2007; **26**: 1663-1670

35 **Fry MM**, Forman MA. 5-fluorouracil toxicity with severe bone marrow suppression in a dog. *Vet Hum Toxicol* 2004; **46**: 178-180

36 **Grenader T**, Goldberg A, Gabizon A. Combination therapy with oxaliplatin and 5-fluorouracil in a patient with severe hepatic dysfunction associated with metastatic adenocarcinoma of the large bowel. *Anticancer Drugs* 2009; **20**: 845-847

37 **Yoshisue K**, Kanie S, Nishimura T, Chikamoto J, Nagayama S. Effect of dimethylnitrosamine-induced liver dysfunction on the pharmacokinetics of 5-fluorouracil after administration of S-1, an antitumour drug, to rats. *J Pharm Pharmacol* 2009; **61**: 1643-1651

38 **Fakih MG**. 5-fluorouracil leucovorin and oxaliplatin (FOLFOX) in the treatment of metastatic colon cancer with severe liver dysfunction. *Oncology* 2004; **67**: 222-224